

Observation of the Baryonic Flavor-Changing Neutral Current Decay $\Lambda_b^0 \rightarrow \Lambda \mu^+ \mu^-$

T. Aaltonen,²² B. Álvarez González^{v,10} S. Amerio,⁴² D. Amidei,³³ A. Anastassov,³⁷ A. Annovi,¹⁸ J. Antos,¹³ G. Apollinari,¹⁶ J.A. Appel,¹⁶ A. Apresyan,⁴⁷ T. Arisawa,⁵⁶ A. Artikov,¹⁴ J. Asaadi,⁵² W. Ashmanskas,¹⁶ B. Auerbach,⁵⁹ A. Aurisano,⁵² F. Azfar,⁴¹ W. Badgett,¹⁶ A. Barbaro-Galtieri,²⁷ V.E. Barnes,⁴⁷ B.A. Barnett,²⁴ P. Barria^{ee,45} P. Bartos,¹³ M. Baucce^{cc,42} G. Bauer,³¹ F. Bedeschi,⁴⁵ D. Beecher,²⁹ S. Behari,²⁴ G. Bellettini^{dd,45} J. Bellinger,⁵⁸ D. Benjamin,¹⁵ A. Beretvas,¹⁶ A. Bhatti,⁴⁹ M. Binkley^{*,16} D. Bisello^{cc,42} I. Bizjak^{ii,29} K.R. Bland,⁵ C. Blocker,⁷ B. Blumenfeld,²⁴ A. Bocci,¹⁵ A. Bodek,⁴⁸ D. Bortoletto,⁴⁷ J. Boudreau,⁴⁶ A. Boveia,¹² B. Brau^{a,16} L. Brigliadori^{bb,6} A. Brisuda,¹³ C. Bromberg,³⁴ E. Brucken,²² M. Bucciantonio^{dd,45} J. Budagov,¹⁴ H.S. Budd,⁴⁸ S. Budd,²³ K. Burkett,¹⁶ G. Busetto^{cc,42} P. Bussey,²⁰ A. Buzatu,³² S. Cabrera^{x,15} C. Calancha,³⁰ S. Camarda,⁴ M. Campanelli,³⁴ M. Campbell,³³ F. Canelli^{12,16} A. Canepa,⁴⁴ B. Carls,²³ D. Carlsmith,⁵⁸ R. Carosi,⁴⁵ S. Carrillo^{k,17} S. Carron,¹⁶ B. Casal,¹⁰ M. Casarsa,¹⁶ A. Castro^{bb,6} P. Catastini,¹⁶ D. Cauz,⁵³ V. Cavaliere^{ee,45} M. Cavalli-Sforza,⁴ A. Cerri^{f,27} L. Cerrito^{q,29} Y.C. Chen,¹ M. Chertok,⁸ G. Chiarelli,⁴⁵ G. Chlachidze,¹⁶ F. Chlebana,¹⁶ K. Cho,²⁶ D. Chokheli,¹⁴ J.P. Chou,²¹ W.H. Chung,⁵⁸ Y.S. Chung,⁴⁸ C.I. Ciobanu,⁴³ M.A. Ciocci^{ee,45} A. Clark,¹⁹ D. Clark,⁷ G. Compostella^{cc,42} M.E. Convery,¹⁶ J. Conway,⁸ M. Corbo,⁴³ M. Cordelli,¹⁸ C.A. Cox,⁸ D.J. Cox,⁸ F. Crescioli^{dd,45} C. Cuenca Almenar,⁵⁹ J. Cuevas^{v,10} R. Culbertson,¹⁶ D. Dagenhart,¹⁶ N. d'Ascenzo^{t,43} M. Datta,¹⁶ P. de Barbaro,⁴⁸ S. De Cecco,⁵⁰ G. De Lorenzo,⁴ M. Dell'Orso^{dd,45} C. Deluca,⁴ L. Demortier,⁴⁹ J. Deng^{c,15} M. Deninno,⁶ F. Devoto,²² M. d'Errico^{cc,42} A. Di Canto^{dd,45} B. Di Ruzza,⁴⁵ J.R. Dittmann,⁵ M. D'Onofrio,²⁸ S. Donati^{dd,45} P. Dong,¹⁶ T. Dorigo,⁴² K. Ebina,⁵⁶ A. Elagin,⁵² A. Eppig,³³ R. Erbacher,⁸ D. Errede,²³ S. Errede,²³ N. Ershaidat^{aa,43} R. Eusebi,⁵² H.C. Fang,²⁷ S. Farrington,⁴¹ M. Feindt,²⁵ J.P. Fernandez,³⁰ C. Ferrazza^{ff,45} R. Field,¹⁷ G. Flanagan^{r,47} R. Forrest,⁸ M.J. Frank,⁵ M. Franklin,²¹ J.C. Freeman,¹⁶ I. Furic,¹⁷ M. Gallinaro,⁴⁹ J. Galyardt,¹¹ J.E. Garcia,¹⁹ A.F. Garfinkel,⁴⁷ P. Garosi^{ee,45} H. Gerberich,²³ E. Gerchtein,¹⁶ S. Giagu^{gg,50} V. Giakoumopoulou,³ P. Giannetti,⁴⁵ K. Gibson,⁴⁶ C.M. Ginsburg,¹⁶ N. Giokaris,³ P. Giromini,¹⁸ M. Giunta,⁴⁵ G. Giurgiu,²⁴ V. Glagolev,¹⁴ D. Glenzinski,¹⁶ M. Gold,³⁶ D. Goldin,⁵² N. Goldschmidt,¹⁷ A. Golossanov,¹⁶ G. Gomez,¹⁰ G. Gomez-Ceballos,³¹ M. Goncharov,³¹ O. González,³⁰ I. Gorelov,³⁶ A.T. Goshaw,¹⁵ K. Goulianos,⁴⁹ A. Gresele,⁴² S. Grinstein,⁴ C. Grosso-Pilcher,¹² R.C. Group,¹⁶ J. Guimaraes da Costa,²¹ Z. Gunay-Unalan,³⁴ C. Haber,²⁷ S.R. Hahn,¹⁶ E. Halkiadakis,⁵¹ A. Hamaguchi,⁴⁰ J.Y. Han,⁴⁸ F. Happacher,¹⁸ K. Hara,⁵⁴ D. Hare,⁵¹ M. Hare,⁵⁵ R.F. Harr,⁵⁷ K. Hatakeyama,⁵ C. Hays,⁴¹ M. Heck,²⁵ J. Heinrich,⁴⁴ M. Herndon,⁵⁸ S. Hewamanage,⁵ D. Hidas,⁵¹ A. Hocker,¹⁶ W. Hopkins^{g,16} D. Horn,²⁵ S. Hou,¹ R.E. Hughes,³⁸ M. Hurwitz,¹² U. Husemann,⁵⁹ N. Hussain,³² M. Hussein,³⁴ J. Huston,³⁴ G. Introzzi,⁴⁵ M. Iori^{gg,50} A. Ivanov^{o,8} E. James,¹⁶ D. Jang,¹¹ B. Jayatilaka,¹⁵ E.J. Jeon,²⁶ M.K. Jha,⁶ S. Jindariani,¹⁶ W. Johnson,⁸ M. Jones,⁴⁷ K.K. Joo,²⁶ S.Y. Jun,¹¹ T.R. Junk,¹⁶ T. Kamon,⁵² P.E. Karchin,⁵⁷ Y. Kato^{n,40} W. Ketchum,¹² J. Keung,⁴⁴ V. Khotilovich,⁵² B. Kilminster,¹⁶ D.H. Kim,²⁶ H.S. Kim,²⁶ H.W. Kim,²⁶ J.E. Kim,²⁶ M.J. Kim,¹⁸ S.B. Kim,²⁶ S.H. Kim,⁵⁴ Y.K. Kim,¹² N. Kimura,⁵⁶ S. Klimentenko,¹⁷ K. Kondo,⁵⁶ D.J. Kong,²⁶ J. Konigsberg,¹⁷ A. Korytov,¹⁷ A.V. Kotwal,¹⁵ M. Kreps,²⁵ J. Kroll,⁴⁴ D. Krop,¹² N. Krumnack^{l,5} M. Kruse,¹⁵ V. Krutelyov^{d,52} T. Kuhr,²⁵ M. Kurata,⁵⁴ S. Kwang,¹² A.T. Laasanen,⁴⁷ S. Lami,⁴⁵ S. Lammel,¹⁶ M. Lancaster,²⁹ R.L. Lander,⁸ K. Lannon^{u,38} A. Lath,⁵¹ G. Latino^{ee,45} I. Lazzizzera,⁴² T. LeCompte,² E. Lee,⁵² H.S. Lee,¹² J.S. Lee,²⁶ S.W. Lee^{w,52} S. Leo^{dd,45} S. Leone,⁴⁵ J.D. Lewis,¹⁶ C.-J. Lin,²⁷ J. Linacre,⁴¹ M. Lindgren,¹⁶ E. Lipeles,⁴⁴ A. Lister,¹⁹ D.O. Litvintsev,¹⁶ C. Liu,⁴⁶ Q. Liu,⁴⁷ T. Liu,¹⁶ S. Lockwitz,⁵⁹ N.S. Lockyer,⁴⁴ A. Loginov,⁵⁹ D. Lucchesi^{cc,42} J. Lueck,²⁵ P. Lujan,²⁷ P. Lukens,¹⁶ G. Lungu,⁴⁹ J. Lys,²⁷ R. Lysak,¹³ R. Madrak,¹⁶ K. Maeshima,¹⁶ K. Makhoul,³¹ P. Maksimovic,²⁴ S. Malik,⁴⁹ G. Manca^{b,28} A. Manousakis-Katsikakis,³ F. Margaroli,⁴⁷ C. Marino,²⁵ M. Martínez,⁴ R. Martínez-Ballarín,³⁰ P. Mastrandrea,⁵⁰ M. Mathis,²⁴ M.E. Mattson,⁵⁷ P. Mazzanti,⁶ K.S. McFarland,⁴⁸ P. McIntyre,⁵² R. McNulty^{i,28} A. Mehta,²⁸ P. Mehtala,²² A. Menzione,⁴⁵ C. Mesropian,⁴⁹ T. Miao,¹⁶ D. Mietlicki,³³ A. Mitra,¹ H. Miyake,⁵⁴ S. Moed,²¹ N. Moggi,⁶ M.N. Mondragon^{k,16} C.S. Moon,²⁶ R. Moore,¹⁶ M.J. Morello,¹⁶ J. Morlock,²⁵ P. Movilla Fernandez,¹⁶ A. Mukherjee,¹⁶ Th. Muller,²⁵ P. Murat,¹⁶ M. Mussini^{bb,6} J. Nachtman^{m,16} Y. Nagai,⁵⁴ J. Naganoma,⁵⁶ I. Nakano,³⁹ A. Napier,⁵⁵ J. Nett,⁵⁸ C. Neu^{z,44} M.S. Neubauer,²³ J. Nielsen^{e,27} L. Nodulman,² O. Norriella,²³ E. Nurse,²⁹ L. Oakes,⁴¹ S.H. Oh,¹⁵ Y.D. Oh,²⁶ I. Oksuzian,¹⁷ T. Okusawa,⁴⁰ R. Orava,²² L. Ortolan,⁴ S. Pagan Griso^{cc,42} C. Pagliarone,⁵³ E. Palencia^{f,10} V. Papadimitriou,¹⁶ A.A. Paramonov,² J. Patrick,¹⁶ G. Pauletta^{hh,53} M. Paulini,¹¹ C. Paus,³¹ D.E. Pellett,⁸ A. Penzo,⁵³ T.J. Phillips,¹⁵ G. Piacentino,⁴⁵ E. Pianori,⁴⁴ J. Pilot,³⁸ K. Pitts,²³ C. Plager,⁹ L. Pondrom,⁵⁸ K. Potamianos,⁴⁷ O. Poukhov^{*,14} F. Prokoshin^{y,14} A. Pronko,¹⁶ F. Ptohos^{h,18} E. Pueschel,¹¹ G. Punzi^{dd,45}

J. Pursley,⁵⁸ A. Rahaman,⁴⁶ V. Ramakrishnan,⁵⁸ N. Ranjan,⁴⁷ I. Redondo,³⁰ P. Renton,⁴¹ M. Rescigno,⁵⁰ F. Rimondi,^{bb,6} L. Ristori,^{45,16} A. Robson,²⁰ T. Rodrigo,¹⁰ T. Rodriguez,⁴⁴ E. Rogers,²³ S. Rolli,⁵⁵ R. Roser,¹⁶ M. Rossi,⁵³ F. Ruffini,^{ee,45} A. Ruiz,¹⁰ J. Russ,¹¹ V. Rusu,¹⁶ A. Safonov,⁵² W.K. Sakumoto,⁴⁸ L. Santi,^{hh,53} L. Sartori,⁴⁵ K. Sato,⁵⁴ V. Saveliev,^{t,43} A. Savoy-Navarro,⁴³ P. Schlabach,¹⁶ A. Schmidt,²⁵ E.E. Schmidt,¹⁶ M.P. Schmidt*,⁵⁹ M. Schmitt,³⁷ T. Schwarz,⁸ L. Scodellaro,¹⁰ A. Scribano,^{ee,45} F. Scuri,⁴⁵ A. Sedov,⁴⁷ S. Seidel,³⁶ Y. Seiya,⁴⁰ A. Semenov,¹⁴ F. Sforza,^{dd,45} A. Sfyrla,²³ S.Z. Shalhout,⁸ T. Shears,²⁸ P.F. Shepard,⁴⁶ M. Shimojima^{s,54} S. Shiraishi,¹² M. Shochet,¹² I. Shreyber,³⁵ A. Simonenko,¹⁴ P. Sinervo,³² A. Sissakian*,¹⁴ K. Sliwa,⁵⁵ J.R. Smith,⁸ F.D. Snider,¹⁶ A. Soha,¹⁶ S. Somalwar,⁵¹ V. Sorin,⁴ P. Squillacioti,¹⁶ M. Stanitzki,⁵⁹ R. St. Denis,²⁰ B. Stelzer,³² O. Stelzer-Chilton,³² D. Stentz,³⁷ J. Strologas,³⁶ G.L. Strycker,³³ Y. Sudo,⁵⁴ A. Sukhanov,¹⁷ I. Suslov,¹⁴ K. Takemasa,⁵⁴ Y. Takeuchi,⁵⁴ J. Tang,¹² M. Tecchio,³³ P.K. Teng,¹ J. Thom^{g,16} J. Thome,¹¹ G.A. Thompson,²³ E. Thomson,⁴⁴ P. Ttito-Guzmán,³⁰ S. Tkaczyk,¹⁶ D. Toback,⁵² S. Tokar,¹³ K. Tollefson,³⁴ T. Tomura,⁵⁴ D. Tonelli,¹⁶ S. Torre,¹⁸ D. Torretta,¹⁶ P. Totaro,^{hh,53} M. Trovato^{ff,45} Y. Tu,⁴⁴ N. Turini^{ee,45} F. Ukegawa,⁵⁴ S. Uozumi,²⁶ A. Varganov,³³ E. Vataga^{ff,45} F. Vázquez^{k,17} G. Velev,¹⁶ C. Vellidis,³ M. Vidal,³⁰ I. Vila,¹⁰ R. Vilar,¹⁰ M. Vogel,³⁶ G. Volpi^{dd,45} P. Wagner,⁴⁴ R.L. Wagner,¹⁶ T. Wakisaka,⁴⁰ R. Wallny,⁹ S.M. Wang,¹ A. Warburton,³² D. Waters,²⁹ M. Weinberger,⁵² H. Wenzel,¹⁶ W.C. Wester III,¹⁶ B. Whitehouse,⁵⁵ D. Whiteson^{c,44} A.B. Wicklund,² E. Wicklund,¹⁶ S. Wilbur,¹² F. Wick,²⁵ H.H. Williams,⁴⁴ J.S. Wilson,³⁸ P. Wilson,¹⁶ B.L. Winer,³⁸ P. Wittich^{g,16} S. Wolbers,¹⁶ H. Wolfe,³⁸ T. Wright,³³ X. Wu,¹⁹ Z. Wu,⁵ K. Yamamoto,⁴⁰ J. Yamaoka,¹⁵ T. Yang,¹⁶ U.K. Yang^{p,12} Y.C. Yang,²⁶ W.-M. Yao,²⁷ G.P. Yeh,¹⁶ K. Yi^{m,16} J. Yoh,¹⁶ K. Yorita,⁵⁶ T. Yoshida^{j,40} G.B. Yu,¹⁵ I. Yu,²⁶ S.S. Yu,¹⁶ J.C. Yun,¹⁶ A. Zanetti,⁵³ Y. Zeng,¹⁵ and S. Zucchelli^{bb6}

(CDF Collaboration[†])

¹*Institute of Physics, Academia Sinica, Taipei, Taiwan 11529, Republic of China*

²*Argonne National Laboratory, Argonne, Illinois 60439, USA*

³*University of Athens, 157 71 Athens, Greece*

⁴*Institut de Física d'Altes Energies, Universitat Autònoma de Barcelona, E-08193, Bellaterra (Barcelona), Spain*

⁵*Baylor University, Waco, Texas 76798, USA*

⁶*Istituto Nazionale di Fisica Nucleare Bologna, ^{bb}University of Bologna, I-40127 Bologna, Italy*

⁷*Brandeis University, Waltham, Massachusetts 02254, USA*

⁸*University of California, Davis, Davis, California 95616, USA*

⁹*University of California, Los Angeles, Los Angeles, California 90024, USA*

¹⁰*Instituto de Física de Cantabria, CSIC-University of Cantabria, 39005 Santander, Spain*

¹¹*Carnegie Mellon University, Pittsburgh, Pennsylvania 15213, USA*

¹²*Enrico Fermi Institute, University of Chicago, Chicago, Illinois 60637, USA*

¹³*Comenius University, 842 48 Bratislava, Slovakia; Institute of Experimental Physics, 040 01 Kosice, Slovakia*

¹⁴*Joint Institute for Nuclear Research, RU-141980 Dubna, Russia*

¹⁵*Duke University, Durham, North Carolina 27708, USA*

¹⁶*Fermi National Accelerator Laboratory, Batavia, Illinois 60510, USA*

¹⁷*University of Florida, Gainesville, Florida 32611, USA*

¹⁸*Laboratori Nazionali di Frascati, Istituto Nazionale di Fisica Nucleare, I-00044 Frascati, Italy*

¹⁹*University of Geneva, CH-1211 Geneva 4, Switzerland*

²⁰*Glasgow University, Glasgow G12 8QQ, United Kingdom*

²¹*Harvard University, Cambridge, Massachusetts 02138, USA*

²²*Division of High Energy Physics, Department of Physics,*

University of Helsinki and Helsinki Institute of Physics, FIN-00014, Helsinki, Finland

²³*University of Illinois, Urbana, Illinois 61801, USA*

²⁴*The Johns Hopkins University, Baltimore, Maryland 21218, USA*

²⁵*Institut für Experimentelle Kernphysik, Karlsruhe Institute of Technology, D-76131 Karlsruhe, Germany*

²⁶*Center for High Energy Physics: Kyungpook National University,*

Daegu 702-701, Korea; Seoul National University, Seoul 151-742,

Korea; Sungkyunkwan University, Suwon 440-746,

Korea; Korea Institute of Science and Technology Information,

Daejeon 305-806, Korea; Chonnam National University, Gwangju 500-757,

Korea; Chonbuk National University, Jeonju 561-756, Korea

²⁷*Ernest Orlando Lawrence Berkeley National Laboratory, Berkeley, California 94720, USA*

²⁸*University of Liverpool, Liverpool L69 7ZE, United Kingdom*

²⁹*University College London, London WC1E 6BT, United Kingdom*

³⁰*Centro de Investigaciones Energeticas Medioambientales y Tecnológicas, E-28040 Madrid, Spain*

³¹*Massachusetts Institute of Technology, Cambridge, Massachusetts 02139, USA*

³²*Institute of Particle Physics: McGill University, Montréal, Québec,*

Canada H3A 2T8; Simon Fraser University, Burnaby, British Columbia,

- Canada V5A 1S6; University of Toronto, Toronto, Ontario,
Canada M5S 1A7; and TRIUMF, Vancouver, British Columbia, Canada V6T 2A3
³³University of Michigan, Ann Arbor, Michigan 48109, USA
³⁴Michigan State University, East Lansing, Michigan 48824, USA
³⁵Institution for Theoretical and Experimental Physics, ITEP, Moscow 117259, Russia
³⁶University of New Mexico, Albuquerque, New Mexico 87131, USA
³⁷Northwestern University, Evanston, Illinois 60208, USA
³⁸The Ohio State University, Columbus, Ohio 43210, USA
³⁹Okayama University, Okayama 700-8530, Japan
⁴⁰Osaka City University, Osaka 588, Japan
⁴¹University of Oxford, Oxford OX1 3RH, United Kingdom
⁴²Istituto Nazionale di Fisica Nucleare, Sezione di Padova-Trento, ^{cc}University of Padova, I-35131 Padova, Italy
⁴³LPNHE, Universite Pierre et Marie Curie/IN2P3-CNRS, UMR7585, Paris, F-75252 France
⁴⁴University of Pennsylvania, Philadelphia, Pennsylvania 19104, USA
⁴⁵Istituto Nazionale di Fisica Nucleare Pisa, ^{dd}University of Pisa,
^{ee}University of Siena and ^{ff}Scuola Normale Superiore, I-56127 Pisa, Italy
⁴⁶Purdue University, Pittsburgh, Pennsylvania 15260, USA
⁴⁷Purdue University, West Lafayette, Indiana 47907, USA
⁴⁸University of Rochester, Rochester, New York 14627, USA
⁴⁹The Rockefeller University, New York, New York 10065, USA
⁵⁰Istituto Nazionale di Fisica Nucleare, Sezione di Roma 1,
^{gg}Sapienza Università di Roma, I-00185 Roma, Italy
⁵¹Rutgers University, Piscataway, New Jersey 08855, USA
⁵²Texas A&M University, College Station, Texas 77843, USA
⁵³Istituto Nazionale di Fisica Nucleare Trieste/Udine,
I-34100 Trieste, ^{hh}University of Trieste/Udine, I-33100 Udine, Italy
⁵⁴University of Tsukuba, Tsukuba, Ibaraki 305, Japan
⁵⁵Tufts University, Medford, Massachusetts 02155, USA
⁵⁶Waseda University, Tokyo 169, Japan
⁵⁷Wayne State University, Detroit, Michigan 48201, USA
⁵⁸University of Wisconsin, Madison, Wisconsin 53706, USA
⁵⁹Yale University, New Haven, Connecticut 06520, USA

We report the first observation of the baryonic flavor-changing neutral current decay $\Lambda_b^0 \rightarrow \Lambda\mu^+\mu^-$ with 24 signal events and a statistical significance of 5.8 Gaussian standard deviations. This measurement uses a $p\bar{p}$ collisions data sample corresponding to 6.8 fb^{-1} at $\sqrt{s} = 1.96 \text{ TeV}$ collected by the CDF II detector at the Tevatron collider. The total and differential branching ratios for $\Lambda_b^0 \rightarrow \Lambda\mu^+\mu^-$ are measured. We find $\mathcal{B}(\Lambda_b^0 \rightarrow \Lambda\mu^+\mu^-) = [1.73 \pm 0.42(\text{stat}) \pm 0.55(\text{syst})] \times 10^{-6}$. We also report the first measurement of the differential branching ratio of $B_s^0 \rightarrow \phi\mu^+\mu^-$ using 49 signal events. In addition, we report branching ratios for $B^+ \rightarrow K^+\mu^+\mu^-$, $B^0 \rightarrow K^0\mu^+\mu^-$ and $B \rightarrow K^*(892)\mu^+\mu^-$ decays.

PACS numbers: 13.25 Hw, 13.20 He, 13.30 -a

*Deceased

†With visitors from ^aUniversity of Massachusetts Amherst, Amherst, Massachusetts 01003, ^bIstituto Nazionale di Fisica Nucleare, Sezione di Cagliari, 09042 Monserrato (Cagliari), Italy, ^cUniversity of California Irvine, Irvine, CA 92697, ^dUniversity of California Santa Barbara, Santa Barbara, CA 93106 ^eUniversity of California Santa Cruz, Santa Cruz, CA 95064, ^fCERN, CH-1211 Geneva, Switzerland, ^gCornell University, Ithaca, NY 14853, ^hUniversity of Cyprus, Nicosia CY-1678, Cyprus, ⁱUniversity College Dublin, Dublin 4, Ireland, ^jUniversity of Fukui, Fukui City, Fukui Prefecture, Japan 910-0017, ^kUniversidad Iberoamericana, Mexico D.F., Mexico, ^lIowa State University, Ames, IA 50011, ^mUniversity of Iowa, Iowa City, IA 52242, ⁿKinki University, Higashi-Osaka City, Japan 577-8502, ^oKansas State University, Manhattan, KS 66506, ^pUniversity of Manchester, Manchester M13 9PL, England, ^qQueen Mary, University of London, London, E1 4NS, England, ^rMuons, Inc., Batavia, IL 60510, ^sNagasaki In-

Rare decays of hadrons containing bottom quarks through the process $b \rightarrow s\mu\mu$, where b is a bottom quark and s is a strange quark, occur in the standard model (SM) with $\mathcal{O}(10^{-6})$ branching ratios [1, 2]. The b and s quarks carry the same charge but different flavor, so this process is a flavor-changing neutral-current (FCNC)

stitute of Applied Science, Nagasaki, Japan, ^tNational Research Nuclear University, Moscow, Russia, ^uUniversity of Notre Dame, Notre Dame, IN 46556, ^vUniversidad de Oviedo, E-33007 Oviedo, Spain, ^wTexas Tech University, Lubbock, TX 79609, ^xIFIC(CSIC-Universitat de Valencia), 56071 Valencia, Spain, ^yUniversidad Tecnica Federico Santa Maria, 110v Valparaiso, Chile, ^zUniversity of Virginia, Charlottesville, VA 22906, ^{aa}Yarmouk University, Irbid 211-63, Jordan, ⁱⁱOn leave from J. Stefan Institute, Ljubljana, Slovenia,

decay. FCNC decays are suppressed at tree level in the SM, and must occur through higher order, and more suppressed, loop diagrams. Their suppressed nature and clean experimental signature, along with reliable theoretical predictions for their rates [1, 3, 4], make them excellent search channels for new physics. With multi-body final states, these modes offer sensitivity to new physics in a number of kinematic distributions in addition to the total branching ratio. In this letter we report measurements of the total branching ratios of FCNC decays, as well as their differential branching ratios as a function of $q^2 \equiv M_{\mu\mu}^2/c^2$. Exclusive decays of $B \rightarrow K^{(*)}\mu^+\mu^-$ have been observed by BABAR [5], Belle [6], and CDF [7]. The CDF experiment also recently reported the observation of $B_s^0 \rightarrow \phi(1020)\mu^+\mu^-$ [7]. No significant departure from the SM has been found thus far.

In addition, the study of the exclusive baryonic $b \rightarrow s\mu\mu$ decays is very important, since theoretical calculation of the exclusive $b \rightarrow s\mu\mu$ decay branching ratio is limited by the uncertainty on the hadronic form factor, and the baryonic decay have different form factors from the mesonic decays. Measurements of both mesonic and baryonic FCNC decays therefore provide complementary tests of the SM and its extensions. However, no b baryon FCNC decay has been observed and there are few experimental constraints on their decay rates. The $\Lambda_b^0 \rightarrow \Lambda\mu^+\mu^-$ decay is considered promising in this respect [8, 9] and experimentally accessible since the branching ratio is predicted as $(4.0 \pm 1.2) \times 10^{-6}$ [9].

The data sample used in the measurements reported in this Letter corresponds to an integrated luminosity of 6.8 fb^{-1} from $p\bar{p}$ collisions at a center-of-mass energy of $\sqrt{s} = 1.96 \text{ TeV}$ collected with the CDF II detector between March 2002 and June 2010. The $\Lambda_b^0 \rightarrow \Lambda\mu^+\mu^-$ decay is reconstructed and measurements are made of the total branching ratio and the differential branching ratio as a function of the dimuon invariant mass squared, q^2 . Besides the updated branching ratios of $B_s^0 \rightarrow \phi\mu^+\mu^-$, $B^+ \rightarrow K^+\mu^+\mu^-$, and $B^0 \rightarrow K^*(892)^0\mu^+\mu^-$, we report the branching ratios of $B^0 \rightarrow K^0\mu^+\mu^-$ and $B^+ \rightarrow K^*(892)^+\mu^+\mu^-$ which are measured for the first time in hadron collisions. We also report the first measurement of the differential branching ratio as a function of q^2 of $B_s^0 \rightarrow \phi\mu^+\mu^-$. To cancel the dominant systematic uncertainties, decay rates for each rare channel $H_b \rightarrow h\mu^+\mu^-$ are measured relative to the corresponding resonant channel $H_b \rightarrow J/\psi h$ with $J/\psi \rightarrow \mu^+\mu^-$, used as a normalization, where H_b represents the b hadron and h stands for Λ , ϕ , K^+ , K_S^0 , K^{*0} , and K^{*+} . Charge-conjugation is implied throughout the Letter.

The reconstruction of the exclusive b hadron events starts with a dimuon sample selected by the online trigger system [10] of the CDF II detector [11]. The trigger system utilizes information from muon detectors and the central outer tracker [12]. Muon chambers CMU and CMX [13] cover $|\eta| < 0.6$ and $0.6 < |\eta| < 1.0$, respec-

tively [14]. The CMP muon chamber covers $|\eta| < 0.6$ and is located behind the CMU and an additional steel absorber. The dimuon trigger requires a pair of oppositely charged muon tracks with a momentum transverse to the beamline, $p_T \geq 1.5 \text{ GeV}/c$ that are matched to track segments in the CMU or CMX chambers. At least one of the muon tracks is required to have a CMU track segment. The trigger also requires that the dimuon pair satisfies either $L_{xy} > 100 \mu\text{m}$, where the transverse decay length L_{xy} is the flight distance between the dimuon vertex and the event primary vertex [15], or $p_T > 3.0 \text{ GeV}/c$ and matched segments in both CMU and CMP chambers for one of the muon candidates.

Offline event selection starts with the triggered dimuon pairs. Each offline track is required to satisfy more stringent requirements on the number of hits used to reconstruct the track. The dimuon selection requirements used in the trigger are repeated with the higher quality offline tracks. The decay length and invariant mass of each dimuon pair are calculated after a vertex fit using the muon tracks. Dimuon pairs are classified according to their invariant mass $M_{\mu\mu}$. Dimuons from FCNC b hadron decays are required to be inconsistent with decaying from J/ψ ($\psi(2S)$) mesons by requiring q^2 values outside the window of $8.68 (12.86) < q^2 < 10.09 (14.18) \text{ GeV}^2/c^2$ [7]. The J/ψ candidates are required to have $M_{\mu\mu}$ within $50 \text{ MeV}/c^2$ of the known J/ψ mass [16].

The $\Lambda_b^0 \rightarrow \Lambda\mu^+\mu^-$ candidates are selected by combining the dimuon pairs with Λ baryons reconstructed from decays $\Lambda \rightarrow p^+\pi^-$. The $p^+\pi^-$ pairs are required to have invariant mass consistent with the known Λ mass [16], $p_T \geq 1.0 \text{ GeV}/c$, and a vertex displaced from the dimuon vertex. The transverse momentum of the Λ_b^0 candidate is required to be greater than $4.0 \text{ GeV}/c$. Candidates with an invariant mass calculated from two or three daughter particles compatible with J/ψ , $\psi(2S)$, D^0 , D^+ , D_s^+ , or Λ_c masses are rejected to remove backgrounds from these charm-hadron decays [7]. The $B_s^0 \rightarrow \phi\mu^+\mu^-$ candidates are reconstructed from dimuons together with a pair of oppositely-charge kaons consistent with a ϕ decay with a selection similar to that of $\Lambda_b^0 \rightarrow \Lambda\mu^+\mu^-$. The $B^{0,+} \rightarrow \mathcal{K}^{0,+}\mu^+\mu^-$ candidates, where $\mathcal{K}^{0,+}$ is one of $\{K^+, K_S^0, K^{*0}, K^{*+}\}$, are formed from a dimuon combined with up to three charged tracks. Details about the reconstruction of the decays of $K^{*0} \rightarrow K^+\pi^-$ and $\phi \rightarrow K^+K^-$ can be found in Ref. [7]. Cross-feed between $\Lambda_b^0 \rightarrow \Lambda\mu^+\mu^-$ and $B^0 \rightarrow K_S^0\mu^+\mu^-$ is suppressed by evaluating the momentum imbalance of Λ and K_S^0 daughters [17]. We remove 76 (90)% of the cross-feed while the signal loss is 11 (7)% for $\Lambda\mu^+\mu^-$ ($K_S^0\mu^+\mu^-$). To further optimize the event selection, an artificial neural network (NN) classifier is trained using simulated signal events and background events taken from mass sidebands in data. Some kinematical distributions of the simulated signal, e.g. transverse momentum of b hadron, and the energy depositions of muon candidates in the electromag-

netic and hadron calorimeters, are corrected using scale factors extracted by comparing simulation to data in the normalization channels. The optimized NN threshold is determined to maximize the significance of the branching ratio, using many kinematic observables including transverse momentum, invariant mass, vertex fit qualities and muon identification qualities [7].

The signal yield of the $\Lambda_b^0 \rightarrow \Lambda\mu^+\mu^-$ candidates is obtained by an unbinned maximum likelihood fit to the Λ_b^0 invariant mass distribution with the signal probability density function (PDF) parametrized by Gaussian distributions using simulated signals and the background PDF modeled by a linear function. The signal region is defined within $\pm 40 \text{ MeV}/c^2$ from the world average Λ_b^0 mass [7]. The statistical significance is obtained through a likelihood-ratio test between the signal plus background and background-only hypotheses interpreted assuming it distributed as a χ^2 variable. The invariant mass distribution of the $\Lambda_b^0 \rightarrow \Lambda\mu^+\mu^-$ candidates is shown in Fig. 1. In the signal region, we observe 24 ± 5 events from $\Lambda_b^0 \rightarrow \Lambda\mu^+\mu^-$ decays while the total number of the signal candidates is 34. The statistical significance of the signal corresponds to 5.8 Gaussian standard deviations. The signal yields of $B_s^0 \rightarrow \phi\mu^+\mu^-$ and other FCNC B meson decays are obtained by similar procedure as that of $\Lambda_b^0 \rightarrow \Lambda\mu^+\mu^-$. Each channel uses independent NN weight and PDF. The fit range for B^+ and B^0 decays is from 5.18 to 5.70 GeV/c^2 to avoid the region of 5.0–5.18 GeV/c^2 , which is dominated by the feed-down background from multi-body decays of b hadrons. While the contribution from charmless H_b decays is negligible due to the muon identification, we estimate a 1% crosstalk between $B^0 \rightarrow K^{*0}\mu^+\mu^-$ and $B_s^0 \rightarrow \phi\mu^+\mu^-$ using simulation, and correct for it. Invariant mass distributions of $B_s^0 \rightarrow \phi\mu^+\mu^-$ and other FCNC B meson decays are shown in Fig. 1 and signal yields are listed in Table I.

TABLE I: Summary of observed yields and the relative efficiency ε_{rel} .

Mode	$N_{h\mu^+\mu^-}$	$N_{J/\psi h}$	ε_{rel}
$\Lambda_b^0 \rightarrow \Lambda\mu^+\mu^-$	24 ± 5	1740 ± 50	0.33 ± 0.01
$B_s^0 \rightarrow \phi\mu^+\mu^-$	49 ± 7	4560 ± 80	0.56 ± 0.01
$B^+ \rightarrow K^+\mu^+\mu^-$	234 ± 19	72200 ± 300	0.41 ± 0.01
$B^0 \rightarrow K^{*0}\mu^+\mu^-$	164 ± 15	28300 ± 200	0.45 ± 0.02
$B^0 \rightarrow K_S^0\mu^+\mu^-$	28 ± 9	9470 ± 90	0.47 ± 0.01
$B^+ \rightarrow K^{*+}\mu^+\mu^-$	20 ± 6	4560 ± 80	0.38 ± 0.02

The branching ratios of $\Lambda_b^0 \rightarrow \Lambda\mu^+\mu^-$, $B_s^0 \rightarrow \phi\mu^+\mu^-$, and $B \rightarrow K^{(*)}\mu^+\mu^-$ are calculated by comparing their signal event yield to that of the normalization decay modes $\Lambda_b^0 \rightarrow J/\psi\Lambda$, $B_s^0 \rightarrow J/\psi\phi$, and $B \rightarrow J/\psi K^{(*)}$, where $J/\psi \rightarrow \mu^+\mu^-$, after the reconstruction efficiency correction:

$$\frac{\mathcal{B}(H_b \rightarrow h\mu^+\mu^-)}{\mathcal{B}(H_b \rightarrow J/\psi h)} = \frac{N_{h\mu^+\mu^-}}{N_{J/\psi h}} \times \frac{\mathcal{B}(J/\psi \rightarrow \mu^+\mu^-)}{\varepsilon_{\text{rel}}}, \quad (1)$$

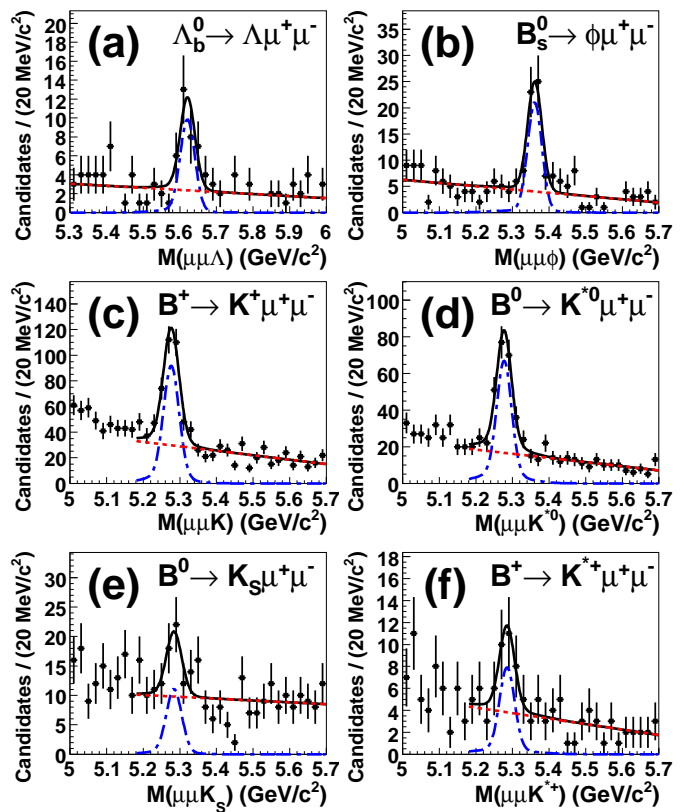


FIG. 1: Invariant mass of (a) $\Lambda_b^0 \rightarrow \Lambda\mu^+\mu^-$, (b) $B_s^0 \rightarrow \phi\mu^+\mu^-$, (c) $B^+ \rightarrow K^+\mu^+\mu^-$, (d) $B^0 \rightarrow K^{*0}\mu^+\mu^-$, (e) $B^0 \rightarrow K_S^0\mu^+\mu^-$, (f) $B^+ \rightarrow K^{*+}\mu^+\mu^-$, with fit results overlaid. The histograms are the data. Solid, dashed-dotted, and dotted curves show the total fit, the signal PDF and the background PDF, respectively.

where $N_{h\mu^+\mu^-}$ is the $h\mu^+\mu^-$ yield, $N_{J/\psi h}$ is the $J/\psi h$ yield for the normalization channel, and $\varepsilon_{\text{rel}} \equiv \varepsilon_{h\mu^+\mu^-} / \varepsilon_{J/\psi h}$ is the relative reconstruction efficiency determined from the simulation. The calculated relative and absolute branching ratios are listed in Table II. The absolute branching ratios are obtained using world averages of the $J/\psi h$ decay rates [16]. The branching ratios of $B^0 \rightarrow K^0\mu^+\mu^-$ and $B^+ \rightarrow K^{*+}\mu^+\mu^-$ are measured for the first time in hadron collisions.

The dominant sources of systematic uncertainty are the scale-factor reweighting of the simulated signal (the trigger efficiency near the threshold) which ranges from 0.5 to 4.0% (0.8 to 7.2%) depending on the channel. We estimate the former uncertainty from the comparison of the relative efficiencies with and without re-weighting and the latter uncertainty from the different p_T requirements for each trigger. In the $\Lambda_b^0 \rightarrow \Lambda\mu^+\mu^-$ case we consider an additional uncertainty of 6.6% due to the unknown $\Lambda_b^0 \rightarrow J/\psi\Lambda$ polarization.

For the absolute branching ratio measurements we assign the uncertainties on the world average $\mathcal{B}(H_b \rightarrow$

$J/\psi h$) [16] or the most recent measurement [18]. Contributions from other sources (e.g. background PDF shape or the decay model of the simulated event) are minor (0.3–1%).

The combined branching ratio is calculated by assuming isospin symmetry and using the B^+ and B^0 total widths [16]. These numbers are consistent with our previous results [7], B -factory measurements [5, 6], and theoretical expectations [8, 9].

TABLE II: Measured branching ratios of rare modes. First (second) uncertainty is statistical (systematic). The last two values are for the isospin average.

Mode	Relative $\mathcal{B}(10^{-3})$	Absolute $\mathcal{B}(10^{-6})$
$\Lambda_b^0 \rightarrow \Lambda \mu^+ \mu^-$	$2.45 \pm 0.59 \pm 0.29$	$1.73 \pm 0.42 \pm 0.55$
$B_s^0 \rightarrow \phi \mu^+ \mu^-$	$1.13 \pm 0.19 \pm 0.07$	$1.47 \pm 0.24 \pm 0.46$
$B^+ \rightarrow K^+ \mu^+ \mu^-$	$0.46 \pm 0.04 \pm 0.02$	$0.46 \pm 0.04 \pm 0.02$
$B^0 \rightarrow K^{*0} \mu^+ \mu^-$	$0.77 \pm 0.08 \pm 0.03$	$1.02 \pm 0.10 \pm 0.06$
$B^0 \rightarrow K^0 \mu^+ \mu^-$	$0.37 \pm 0.12 \pm 0.02$	$0.32 \pm 0.10 \pm 0.02$
$B^+ \rightarrow K^{*+} \mu^+ \mu^-$	$0.67 \pm 0.22 \pm 0.04$	$0.95 \pm 0.32 \pm 0.08$
$B \rightarrow K \mu^+ \mu^-$	–	$0.42 \pm 0.04 \pm 0.02$
$B \rightarrow K^* \mu^+ \mu^-$	–	$1.01 \pm 0.10 \pm 0.05$

We also measure differential branching ratios with respect to the dimuon mass. We divide the signal region into six bins in q^2 . We fit the signal yield in each q^2 bin. In each fit, we fix the mean of the H_b mass and the background slope to the value from the global fit, so that only the signal fraction is allowed to vary in the fit. Figure 2 shows the differential branching ratios for $\Lambda_b^0 \rightarrow \Lambda \mu^+ \mu^-$, $B_s^0 \rightarrow \phi \mu^+ \mu^-$, and $B \rightarrow K^{(*)} \mu^+ \mu^-$. For illustration, we superimpose the SM expectations which are based on the formula in Ref. [1] with the form factors in Ref. [19], except for the case of $\Lambda_b^0 \rightarrow \Lambda \mu^+ \mu^-$ decays which follows Ref. [9]. The discontinuous structure at $q^2 \sim 7 \text{ GeV}^2/c^2$ is due to a change in parameter approximations. Tables III and IV summarize the differential branching ratio measurements. The two bottom rows in each table show the results for the semi-inclusive bins which are included with ranges covering theoretically well-controlled regions.

In summary, we have updated our previous analysis of the flavor-changing neutral current decays $b \rightarrow s \mu \mu$ using data corresponding to an integrated luminosity of 6.8 fb^{-1} and adding new decay channels. We report the first observation of $\Lambda_b^0 \rightarrow \Lambda \mu^+ \mu^-$ and measure the total and differential branching ratios of this decay with respect to q^2 . We also measure the total and differential branching ratios of $B \rightarrow K^{(*)} \mu^+ \mu^-$ and $B_s^0 \rightarrow \phi \mu^+ \mu^-$, with respect to q^2 . All measurements are consistent and competitive with other results, and the differential measurements of $B_s^0 \rightarrow \phi \mu^+ \mu^-$ and $\Lambda_b^0 \rightarrow \Lambda \mu^+ \mu^-$ are the first such measurements. At present there is no evidence of discrepancy from the SM prediction.

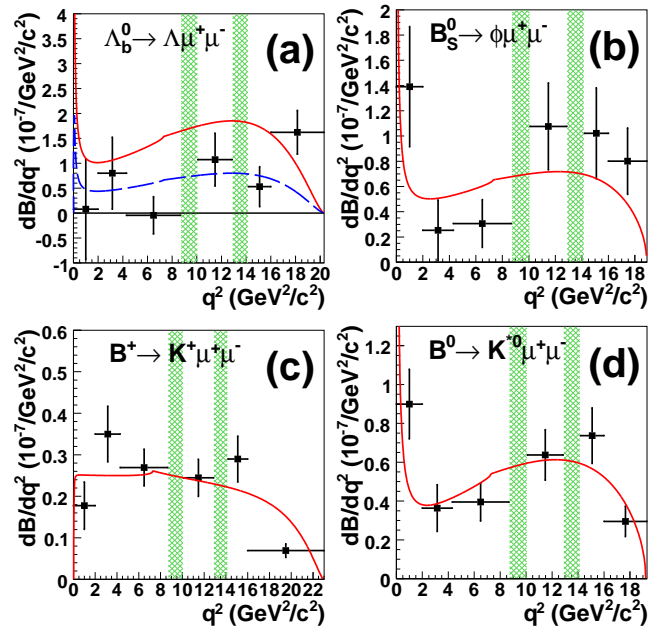


FIG. 2: Differential branching ratios of (a) $\Lambda_b^0 \rightarrow \Lambda \mu^+ \mu^-$, (b) $B_s^0 \rightarrow \phi \mu^+ \mu^-$, (c) $B^+ \rightarrow K^+ \mu^+ \mu^-$, and (d) $B^0 \rightarrow K^{*0} \mu^+ \mu^-$. The points are the fit result. The solid curves are the SM expectation [1, 9, 19]. The dashed line in the $\Lambda_b^0 \rightarrow \Lambda \mu^+ \mu^-$ plot is the SM prediction normalized to our total branching ratio measurement. The hatched regions are the charmonium veto regions.

We thank the Fermilab staff and the technical staffs of the participating institutions for their vital contributions. This work was supported by the U.S. Department of Energy and National Science Foundation; the Italian Istituto Nazionale di Fisica Nucleare; the Ministry of Education, Culture, Sports, Science and Technology of Japan; the Natural Sciences and Engineering Research Council of Canada; the National Science Council of the Republic of China; the Swiss National Science Foundation; the A.P. Sloan Foundation; the Bundesministerium für Bildung und Forschung, Germany; the World Class University Program, the National Research Foundation of Korea; the Science and Technology Facilities Council and the Royal Society, UK; the Institut National de Physique Nucleaire et Physique des Particules/CNRS; the Russian Foundation for Basic Research; the Ministerio de Ciencia e Innovación, and Programa Consolider-Ingenio 2010, Spain; the Slovak R&D Agency; and the Academy of Finland.

- [1] A. Ali *et al.*, Phys. Rev. D **61**, 074024 (2000).
- [2] D. Melikhov, N. Nikitin, and S. Simula, Phys. Rev. D **57**, 6814 (1998).
- [3] Q. Chan and Y.-H. Gao, Nucl. Phys. **B845**, 179 (2011).

TABLE III: Differential branching ratios of $\Lambda_b^0 \rightarrow \Lambda\mu^+\mu^-$, $B^+ \rightarrow K^+\mu^+\mu^-$, $B^0 \rightarrow K^0\mu^+\mu^-$, combined $B \rightarrow K\mu^+\mu^-$, in units of 10^{-7} . The q_{max}^2 is 20.30 (23.00) GeV^2/c^2 for $\Lambda\mu^+\mu^-$ ($K\mu^+\mu^-$). The first (second) uncertainty is statistical (systematic).

q^2 (GeV^2/c^2)	$\Lambda_b^0 \rightarrow \Lambda\mu^+\mu^-$	$B^+ \rightarrow K^+\mu^+\mu^-$	$B^0 \rightarrow K^0\mu^+\mu^-$	$B \rightarrow K\mu^+\mu^-$
[0.00, 2.00]	$0.15 \pm 2.01 \pm 0.05$	$0.36 \pm 0.11 \pm 0.02$	$0.312 \pm 0.372 \pm 0.023$	$0.33 \pm 0.10 \pm 0.02$
[2.00, 4.30]	$1.84 \pm 1.66 \pm 0.59$	$0.80 \pm 0.15 \pm 0.05$	$0.929 \pm 0.485 \pm 0.070$	$0.77 \pm 0.14 \pm 0.04$
[4.30, 8.68]	$-0.20 \pm 1.64 \pm 0.06$	$1.18 \pm 0.19 \pm 0.07$	$0.663 \pm 0.510 \pm 0.050$	$1.05 \pm 0.17 \pm 0.06$
[10.09, 12.86]	$2.97 \pm 1.47 \pm 0.95$	$0.68 \pm 0.12 \pm 0.04$	$-0.030 \pm 0.223 \pm 0.002$	$0.48 \pm 0.10 \pm 0.03$
[14.18, 16.00]	$0.96 \pm 0.73 \pm 0.31$	$0.53 \pm 0.10 \pm 0.03$	$0.726 \pm 0.257 \pm 0.054$	$0.52 \pm 0.09 \pm 0.03$
[16.00, q_{max}^2]	$6.97 \pm 1.88 \pm 2.23$	$0.48 \pm 0.11 \pm 0.03$	$0.214 \pm 0.182 \pm 0.016$	$0.38 \pm 0.09 \pm 0.02$
[0.00, 4.30]	$2.65 \pm 2.52 \pm 0.85$	$1.13 \pm 0.19 \pm 0.07$	$1.268 \pm 0.622 \pm 0.095$	$1.07 \pm 0.17 \pm 0.06$
[1.00, 6.00]	$1.27 \pm 2.08 \pm 0.41$	$1.41 \pm 0.20 \pm 0.09$	$0.980 \pm 0.614 \pm 0.074$	$1.29 \pm 0.18 \pm 0.08$

TABLE IV: Differential branching ratios of $B_s^0 \rightarrow \phi\mu^+\mu^-$, $B^0 \rightarrow K^{*0}\mu^+\mu^-$, $B^+ \rightarrow K^{*+}\mu^+\mu^-$, and combined $B \rightarrow K^*\mu^+\mu^-$, in units of 10^{-7} . The q_{max}^2 is 18.90 (19.30) GeV^2/c^2 for $\phi\mu^+\mu^-$ ($K^*\mu^+\mu^-$). The first (second) uncertainty is statistical (systematic).

q^2 (GeV^2/c^2)	$B_s^0 \rightarrow \phi\mu^+\mu^-$	$B^0 \rightarrow K^{*0}\mu^+\mu^-$	$B^+ \rightarrow K^{*+}\mu^+\mu^-$	$B \rightarrow K^*\mu^+\mu^-$
[0.00, 2.00]	$2.78 \pm 0.95 \pm 0.89$	$1.80 \pm 0.36 \pm 0.11$	$1.30 \pm 0.98 \pm 0.11$	$1.73 \pm 0.33 \pm 0.09$
[2.00, 4.30]	$0.58 \pm 0.55 \pm 0.19$	$0.84 \pm 0.28 \pm 0.05$	$0.71 \pm 1.00 \pm 0.06$	$0.82 \pm 0.26 \pm 0.05$
[4.30, 8.68]	$1.34 \pm 0.83 \pm 0.43$	$1.73 \pm 0.43 \pm 0.10$	$1.71 \pm 1.58 \pm 0.14$	$1.72 \pm 0.41 \pm 0.09$
[10.09, 12.86]	$2.98 \pm 0.95 \pm 0.95$	$1.77 \pm 0.36 \pm 0.10$	$1.97 \pm 0.99 \pm 0.17$	$1.77 \pm 0.34 \pm 0.09$
[14.18, 16.00]	$1.86 \pm 0.66 \pm 0.59$	$1.34 \pm 0.26 \pm 0.08$	$0.52 \pm 0.61 \pm 0.04$	$1.21 \pm 0.24 \pm 0.07$
[16.00, q_{max}^2]	$2.32 \pm 0.76 \pm 0.74$	$0.97 \pm 0.26 \pm 0.06$	$1.57 \pm 0.96 \pm 0.13$	$0.88 \pm 0.22 \pm 0.05$
[0.00, 4.30]	$3.30 \pm 1.09 \pm 1.05$	$2.60 \pm 0.45 \pm 0.15$	$2.01 \pm 1.39 \pm 0.17$	$2.53 \pm 0.43 \pm 0.14$
[1.00, 6.00]	$1.14 \pm 0.79 \pm 0.36$	$1.42 \pm 0.41 \pm 0.08$	$2.57 \pm 1.61 \pm 0.22$	$1.48 \pm 0.39 \pm 0.08$

- [4] Y.-M. Wang, M. J. Aslam, and C.-D. Lu, Eur. Phys. J. C **59**, 847 (2009).
- [5] B. Aubert *et al.* (BaBar Collaboration), Phys. Rev. Lett. **102**, 091803 (2009).
- [6] J. T. Wei *et al.* (Belle Collaboration), Phys. Rev. Lett. **103**, 171801 (2009).
- [7] T. Aaltonen *et al.* (CDF Collaboration), Phys. Rev. Lett. **106**, 161801 (2011).
- [8] C.-H. Chen and C. Q. Geng, Phys. Rev. D **64**, 074001 (2001).
- [9] T. M. Aliev, K. Azizi, and M. Savci, Phys. Rev. D **81**, 056006 (2010).
- [10] E. J. Thomson *et al.*, IEEE Trans. Nucl. Sci. **49**, 1063 (2002).
- [11] D. Acosta *et al.* (CDF Collaboration), Phys. Rev. D **71**, 032001 (2005).
- [12] T. Aaltonen *et al.* (CDF Collaboration), Phys. Rev. Lett. **102**, 242002 (2009), and references therein.
- [13] G. Ascoli *et al.*, Nucl. Instrum. Meth. A **268**, 33 (1988); T. Dorigo (CDF Collaboration), Nucl. Instrum. Meth. A **461**, 560 (2001).
- [14] We use a cylindrical coordinate system in which θ is the polar angle with respect to the proton beamline and pseudorapidity $\eta \equiv -\ln(\tan \theta/2)$.
- [15] W. Ashmanskas *et al.*, Nucl. Instrum. Methods A **518**, 532 (2004).
- [16] K. Nakamura *et al.* (Particle Data Group), J. Phys. G **37**, 075021 (2010).
- [17] J. Podolanski and R. Armenteros, Phil. Mag. **45**, 13 (1954).
- [18] V. M. Abazov *et al.* (D0 Collaboration), arXiv:1105.0690 (2011).
- [19] P. Ball and R. Zwicky, Phys. Rev. D **71**, 014015 (2005); P. Ball and R. Zwicky, Phys. Rev. D **71**, 014029 (2005).